Small mounded contourite drifts associated with deep-water coral banks, Porcupine Seabight, NE Atlantic Ocean

D. VAN ROOIJ[1], D. BLAMART[2], M. KOZACHENKO[3] & J.-P. HENRIET[1]

[1]*Renard Centre of Marine Geology, Ghent University, Krijgslaan 281 S8, B-9000 Gent, Belgium (e-mail: David.VanRooij@UGent.be)*

[2]*Laboratoire des Sciences de Climat et de l'Environnement, Laboratoire mixte CNRS/CEA, Bâtiment 12, 4 avenue de la Terrasse, F-91198 Gif-sur-Yvette, France*

[3]*Coastal and Marine Resources Centre, University College Cork, Cork, Ireland*

Abstract: Numerous studies on sediment drifts have demonstrated a close interaction between sea-bed morphology, palaeoceanography, sediment supply and climate. Contourites have been reported in areas along continental margins directly influenced by the effect of intensive deep-water currents from the global conveyor belt. In this paper, we report the occurrence of a small-scale confined contourite drift from Porcupine Seabight, SW of Ireland, and its association with a province of coral banks. The Porcupine Basin is a relatively shallow, semi-enclosed basin characterized by the presence of cold-water coral bank provinces. These coral banks are often associated to a strong northward-flowing bottom current, created and steered by a complex interaction of the water mass characteristics, tidal influences and sea-bed morphology. Very high-resolution seismic stratigraphy allowed the identification of a small mounded drift, located between a depression created by (1) an irregular palaeotopography caused by a vigorous Late Pliocene erosion event and (2) a north–south alignment of coral banks. Core MD99-2327, taken on the flank of this drift mound, shows the variability of the bottom currents. Sortable silt data show several periods of bottom-current enhancement, which may be linked with warmer periods and an inferred influx of Mediterranean Outflow Water. The glacial part of the core has been interpreted as a muddy contourite with a high content of ice-rafted debris. The lower part of the core is a deep-water massive contourite sand resembling the present-day sea-floor sediments.

The Porcupine Seabight (PSB) is a shallow to deep-water, amphitheatre-shaped basin SW of Ireland, forming a small bight along the North Atlantic margin (Fig. 1). It is the surface expression of the underlying deep sedimentary Porcupine Basin, which is a failed rift of the proto-North Atlantic Ocean, filled with a 10 km thick series of Mesozoic and Cenozoic sediments (Moore & Shannon 1991). The PSB has gained interest because of the presence of special deep-water habitats (Henriet *et al.* 1998; De Mol *et al.* 2002; Huvenne *et al*. 2003), consisting of a province of coral banks, discovered on the eastern slope and described as the Belgica mound province (BMP). Earlier studies (De Mol *et al*. 2002; Huvenne *et al*. 2002; Van Rooij *et al*. 2003) suggested that the geometry of the most recent deposits in this province seemed to be under the influence of bottom currents of variable intensity.

This paper will illustrate the importance of such a relatively small basin as the Porcupine Seabight for the study of bottom-current deposits. Until now, only the large sediment drift systems in the Northern Atlantic Ocean have been extensively studied. High-resolution seismic surveys have allowed description of the details of smaller depositional systems, which were ignored or not observed in earlier studies. In this way, smaller-scale varieties of current-driven deposits were recognized, adding to the complexity of the contourite paradigm (Faugères *et al*. 1999; Rebesco & Stow 2001). Moreover, the local hydrodynamic environment of these deposits may be very complex. Because they mostly are located out of reach of the typical thermohaline deep-sea bottom-current circulation, the driving current process needs to be better understood.

Here, we present and discuss high-resolution seismic and core data. More specifically, this paper highlights the special present and past hydrodynamic environments of the BMP. The role of palaeoceanographic turnovers is discussed in view of the creation of a specific hydrodynamic, morphological and sedimentary environment, ready to host the development of a contourite drift. In addition, the presence of the deep-water coral bank and its interaction with the sedimentary environment is discussed as a controlling key factor. Ultimately, a link between the sedimentary record and past climate changes is proposed.

From: VIANA, A. R. & REBESCO, M. (eds) *Economic and Palaeoceanographic Significance of Contourite Deposits*. Geological Society, London, Special Publications, **276**, 225–244.
0305-8719/07/$15.00

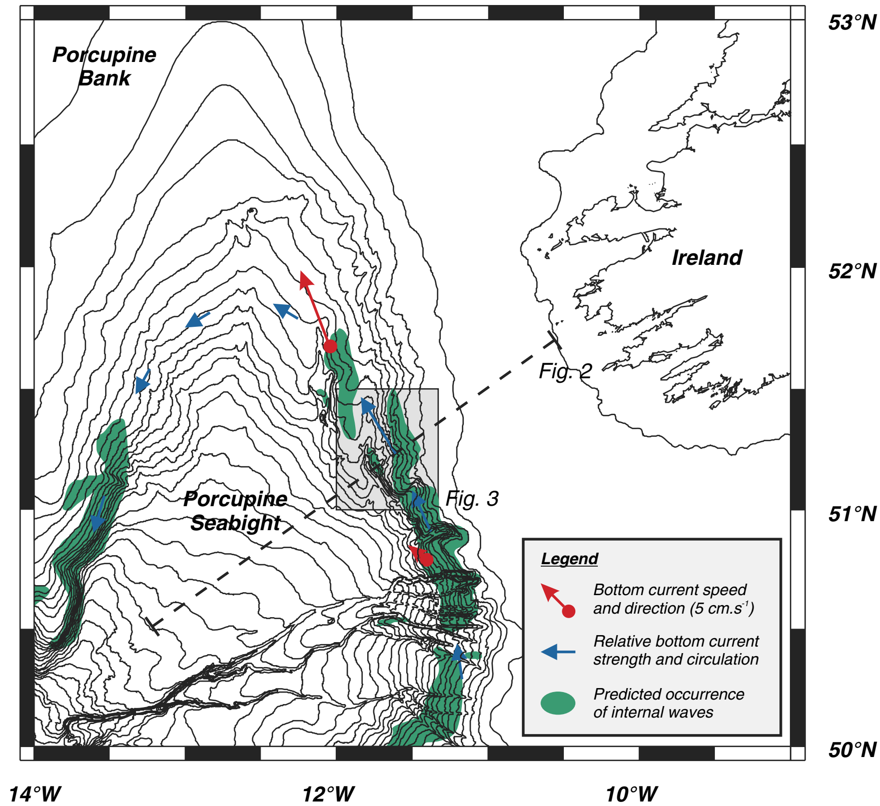

Fig. 1. Location map of the Porcupine Seabight, illustrating the main morphological elements and hydrographic features. The red arrows indicate known general near-bottom current measurements after Pingree & Le Cann (1989); the blue arrows show the assumed general circulation after White (2006). The green areas delineate the predicted occurrence of bottom-current enhancement as a result of internal tides (Rice *et al.* 1990). The GEBCO bathymetry contour intervals are drawn at 100 m intervals.

Material and methods

Very high-resolution seismic profiles

From 1997 to 2003, about 1500 km of single-channel seismic reflection data were collected over the eastern flank of the PSB. These data were acquired with an SIG surface sparker source and recorded with a single-channel surface streamer (vertical resolution between 0.4 and 1 m). These data were recorded digitally using the ELICS Delph 2 system. The basic data processing involved a first, broad-window Butterworth bandpass filter (200 Hz with a 24 dB per octave slope and 2000 Hz with a 36 dB per octave slope), minimum phase predictive deconvolution (with a 20 ms window), followed by a second Butterworth bandpass filter (250 Hz with a 24 dB per octave slope and 700 Hz with a 36 dB per octave slope). Additionally, a true amplitude recovery or an automatic gain control was applied. The obtained network of profiles is organized in a general N60° orientation, running perpendicular to the slope. The distance between adjacent profiles was about 3 km. Only a limited number of long, along-slope (N155°) profiles have been acquired.

Core analyses

Two cores, MD99-2327 and MD01-2449, were analysed for gamma density (g cm^{-3}) and magnetic susceptibility (SI). Grain-size analysis were performed every 5 cm using a Coulter LS130, to provide mean grain size (μm) and sorting (μm). Only core MD99-2327 was analysed for its sortable silt content, at a sample interval of 10 cm. This silt-sized fraction, between 10 and 63 μm, is considered as an indicator of relative bottom-current strength, as bottom currents sort coarse silt during events of resuspension and ensuing deposition.

Stronger currents yield a coarser mean size of the non-cohesive silt fraction, acting through both selective deposition and winnowing (McCave *et al*. 1995).

Core MD99-2327 was also sampled every 10 cm to obtain the coarse sand fraction with a grain size >150 μm and the relative abundance of the planktonic foraminifer *N. pachyderma (s.)* (NPS). A $\delta^{18}O$ stratigraphy for this core was obtained from 10–20 tests of *N. pachyderma (s.)*. The analyses were performed at the LSCE (Gif-sur-Yvette, France) using a VG Optima mass spectrometer equipped with a 'Kiel device' for automatic acidification of individual samples. The isotopic values are reported as per mil deviation with respect to the international V-PDB standard. The uncertainties on the isotope measurements are 0.08‰. Additionally, accelerator mass spectrometry ^{14}C dates were obtained on two monospecific samples of *N. pachyderma (s.)* at 90 and 440 cm downcore. These analyses were also performed at the LSCE and have been corrected for a mean reservoir age of 400 years (Bard 1998).

Hydrography

The present-day water masses of the Porcupine Seabight are in two broad categories: upper water from 0 to 1200 m and deeper water below (Fig. 2). The upper water has sources in the western Atlantic Ocean and the Mediterranean Sea. A permanent thermocline is found from 600 to 1400 m water depth; in this interval the temperature decreases from 10 °C to 4 °C. A seasonal thermocline is formed at about 50 m depth. Within the upper 700 m, the North Atlantic Central Water (NACW) is considered as a saline, winter mode water, formed by strong cooling of water masses NW of Spain (Pollard *et al.* 1996; Van Aken 2000). This winter cooling makes the Eastern North Atlantic Water (ENAW) denser and more saline than NACW. The Mediterranean Outflow Water (MOW) is observed between 700 and 1200 m (White 2006). According to Van Aken (2000), New *et al*. (2001) and White *et al*. (2005), the northward spreading of the MOW occurs as a reasonably steady boundary undercurrent that flows from the Gulf of Cadiz, at least as far as the PSB. Its continuation northward is considered as less certain. The deeper water is characterized by the presence of water masses derived from the Labrador Sea Water (LSW) from 1200 to 1800 m, and North East Atlantic Deep Water (NEADW) with contributions of Norwegian Sea Water (NSW), and is weakly influenced by Antarctic Bottom Water (AABW) (Hargreaves 1984; Rice *et al*. 1991).

A Shelf Edge Current (SEC) is known to be present along the eastern North Atlantic slope, from the Iberian margin to the Norwegian Sea (Pingree & Le Cann 1989, 1990; Rice *et al*. 1991; New *et al.* 2001), carrying warm and saline upper-layer ENAW over the mid-slope in the top 400–500 m (Fig. 2). Within the PSB, a mean northward current is less readily observed, except by near-bottom current meters on the eastern flank. Here, currents are predicted to be strongest at the mid-slope at about 500–600 m (Fig. 1). These bottom currents, with a strong semidiurnal to diurnal tidal

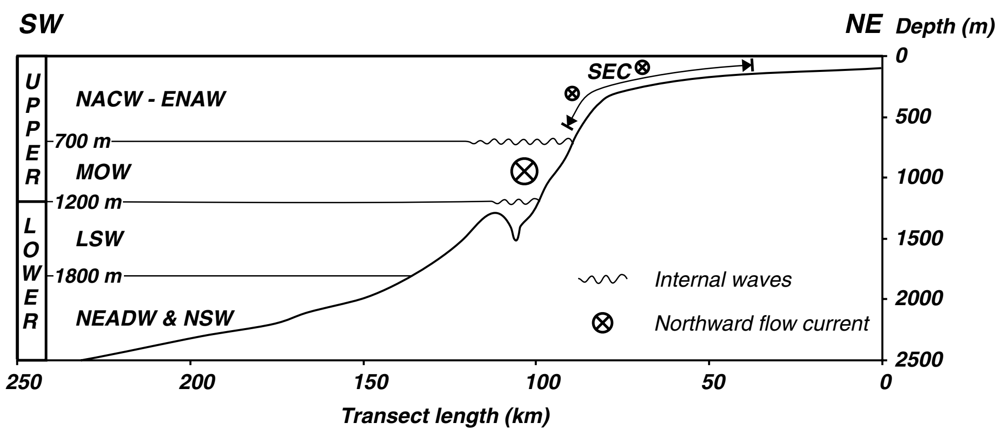

Fig. 2. Compilation of the water stratification along a NE–SW bathymetric transect along the Porcupine Seabight, with indication of the major hydrodynamic processes, after Hargreaves (1984), Rice *et al.* (1990, 1991) and White (2006). The location of this transect is shown in Figure 1. SEC, shelf edge current; NACW, North Atlantic Central Water; ENAW, Eastern North Atlantic Water; MOW, Mediterranean Outflow Water; LSW, Labrador Sea Water; NEADW, North East Atlantic Deep Water; NSW, Norwegian Sea Water.

variation, are strongly steered by the bottom topography (Pingree & Le Cann 1989, 1990; Rice *et al*. 1991). Mean flows of this predominant cyclonic circulation vary between 2 and 5 cm s^{-1} and may reach 10 cm s^{-1}. At the northern end of the PSB, the currents are relatively weaker, flowing towards an anticlockwise pattern around the northern slope (White 2006).

Moreover, Rice *et al*. (1990) and De Mol *et al*. (2002) have suggested that internal tides at a depth between 500 and 1000 m may be responsible for further enhancement of the bottom currents. These are internal waves with tidal periods, generated by the interaction of tidal currents, water stratification and bottom topography. The greatest enhancement is to be expected near the upper boundaries of the interacting water masses, where mixing will occur (Pingree & Le Cann 1989). This occurs predominantly on the eastern flank of the PSB (Fig. 1), where one can expect near-bottom currents estimated at 15–20 cm s^{-1}.

On the eastern slope of the PSB, Kenyon *et al*. (1998) and Wheeler *et al*. (2000) identified current-induced bedforms such as barchan sandwaves, sand ribbons and obstacle marks on high-resolution side-scan sonar imagery. Some of these bedforms indicate that the peak current can reach a considerable speed up to 100 cm s^{-1}. Foubert *et al*. (2005) found visual evidence of this strong hydrodynamic regime using remotely operated vehicle (ROV) submersible investigations. The presence of gravels and boulders within the vicinity of the BMP is very common and some of them are colonized by *Bathylasma* sp. barnacles, indicating strong currents. Sandwaves and superimposed ripples observed on the ROV microbathymetry indicate strong northward currents up to 65 cm s^{-1}. Also, long north–south lineated features with a length up to 250 m can be caused by strong currents of about 150 cm s^{-1}. This is confirmed by direct current measurements at nearby moorings (White *et al.* 2005).

Seismic stratigraphic units

The locations of the seismic lines and cores presented in this study are shown in Figure 3. The sediment drift is located in the central part of the Belgica mound province (Fig. 4). Between the individual coral banks, SW-oriented gullies can be observed. Upslope, another elongated mounded feature is observed, with a relief of *c*. 50–60 m above the sea floor, of 12 km length and maximum 4 km width. At its eastern side, this sediment body is limited by a (north–south elongated) moat channel, which seems to be, in turn, flanked by large south–north elongated scarp. The following section will discuss the internal structure of this sediment body and provide more insight into its construction.

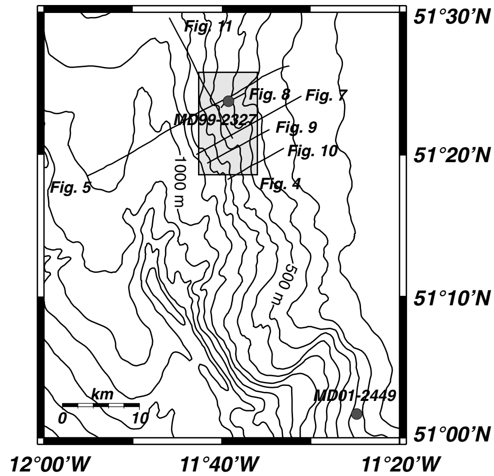

Fig. 3. Map showing the location of the seismic lines, cores (circles) and detailed shaded relief multibeam bathymetry. The GEBCO bathymetry contour intervals are drawn at 100 m intervals.

Pre-contourite drift units (U2–U4)

The stratigraphic record of this area is composed of four units (U4–U1) (Van Rooij *et al*. 2003). The lower boundary of the Quaternary unit U1 is very irregular and is characterized by incisions into underlying units, steep scarps and the presence of coral banks (Fig. 5). These palaeomorphological elements prior to the deposition of U1 are represented in Figure 6.

The acoustically nearly transparent unit U2 has been very heavily incised (Figs 6 and 7). This unit has a limited lateral extent, shows an irregular distribution and is present in two large zones, separated by a large north–south erosional channel (Figs 5 and 6). Generally it disappears towards the NNW and the SW, whereas it extends beyond the data coverage in the northeastern and southeastern part of the study area, where it reaches its maximum thickness of over 200 ms two-way travel time (TWT) (Fig. 6). Several zones have been identified where the thickness of U2 dramatically drops from *c*. 100 ms TWT to 0 ms TWT over about 350 m, creating relatively steep (*c*. 15°) flanks (Fig. 7). Several profiles show the presence of unit U2 at the western side of the erosional channel, still with the same dip as on the eastern side (Fig. 5). The boundary between units U2 and U3 can easily be correlated from one side of the channel to the other. These features strongly

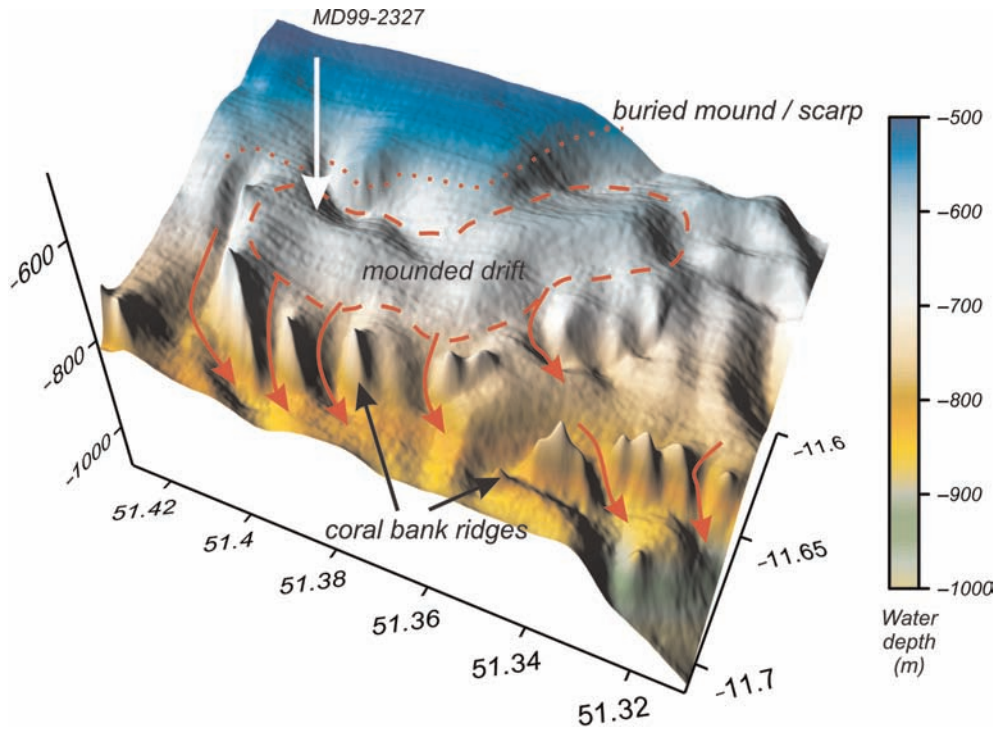

Fig. 4. Surface 3D multibeam bathymetry of the small mounded drift (red dashed lines) with the position of core MD99-2327. The downslope running gullies flanking the coral banks are indicated by the red arrows. The position of the (buried) U2 scarp is indicated by a red dotted line.

suggest that the sediments of unit U2 were deposited over the entire slope and later eroded. Although we have no lithological information on this acoustically transparent unit, its distribution and the seismic facies hint that it might contain very homogeneous sediments.

After the deposition of unit U2, a major change in oceanographic conditions was responsible for a large-scale erosive event along the entire slope of the PSB, leaving a very irregular terrace-like palaeotopography. These deep incisions into unit U2, as well as some U3 strata, created large roughly south–north-oriented ridges with steep flanks (Fig. 6), still evident in the present-day topography (Fig. 4). The timing for this regional hiatus, named RD1, is estimated to be Late Pliocene. It is interpreted in terms of the reintroduction of MOW in the NE Atlantic and the effect of glacial–interglacial events on deep-water circulation (Stow 1982; Pearson & Jenkins 1986).

The Belgica mounds occur in a very narrow bathymetric interval between 700 and 1000 m below sea level, aligned as along-slope-oriented ridges. Most of the observations confirm that these coral banks occupy an elevated position in the palaeobathymetry and are rooted on a scarp or a topographic irregularity corresponding to the RD1 unconformity (Figs 8–10). To the north, the coral banks tend to step off the eroded U2 unit (Figs 6 and 11). In this case, they are resting on a scarp of U3 deposits. Freiwald *et al*. (1999) and De Mol *et al*. (2002) have pointed out that the builders of these coral banks, most often *Lophelia pertusa* and *Madrepora occulata*, prefer to settle on a hard substratum in an elevated position. They need strong bottom currents to obtain sufficient nutrients, and to keep them free from sediment burial. The mere presence of the coral banks may therefore be an indicator of (strong) bottom currents after the Late Pliocene erosion. Moreover, exactly underneath the coral banks, a zone of sigmoidal reflectors observed in unit U3 can be interpreted as sediment waves. Ediger *et al*. (2002), for example, described a similar set of sediment waves in the Mediterranean Cilician basin, migrating upslope in an opposite direction to the present water circulation pattern. This implies the presence of a presumably north- to NW-flowing bottom current on this part

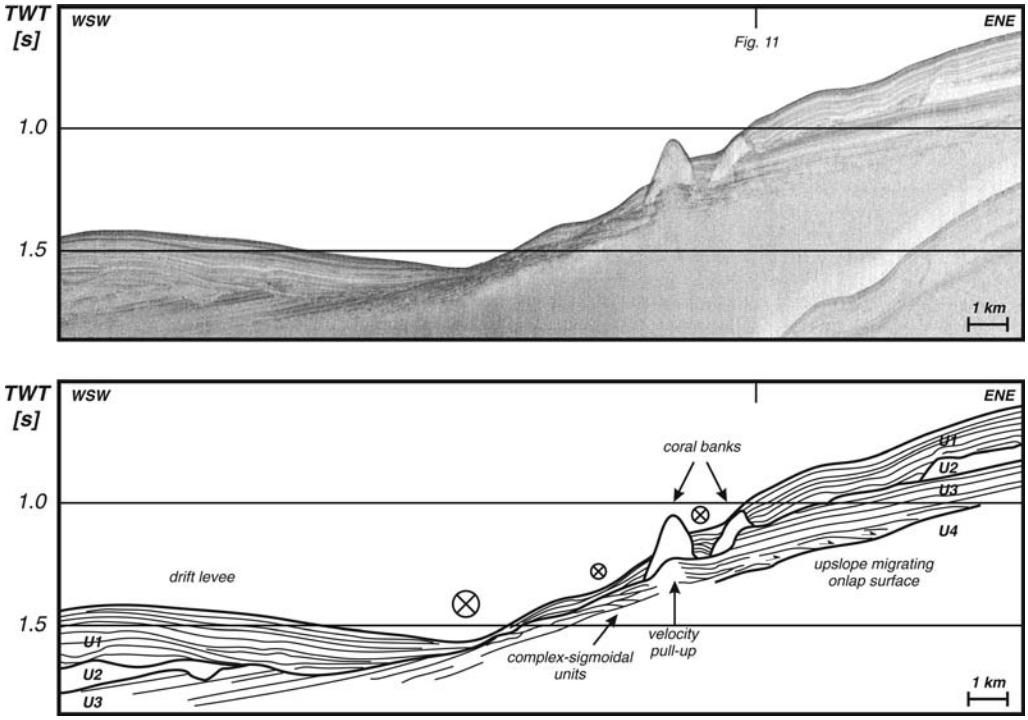

Fig. 5. Profile P980521, illustrating the general seismic stratigraphic setting and showing two coral banks and general sediment drift properties. The several erosional steps along the lower boundary of unit U1 and the incision into unit U3 at the WSW flank of the channel should also be noted.

of the slope during the Early Miocene. If this is the case, this slope section may have been under the influence of enhanced bottom currents since the beginning of the Neogene.

Small mounded contourite drift (U1)

Between the coral banks and the irregular palaeotopography created by the RD1 erosion, reflectors of unit U1 show a mounded feature with a moderate ENE progradation (a; Figs 7 and 9). All the seismic profiles in the study area display a very typical vertical stacking of seismic facies, mainly characterized by changing amplitudes (Figs 7, 10 and 11). The internal geometry of unit U1 seems to be controlled by the length of the passage between the steep flanks of the coral bank and the U2 scarp. In Figure 5, the distance of this passage exceeds 5 km and an undulating–sheeted geometry is observed within unit U1. Only minor irregularities such as downlap features are found against the lower boundary. Figures 7, 9 and 10 on the other hand, show a relatively narrow passage (2 km or less) and the overall geometry of unit U1 shows a mounded appearance with moats on both sides (a). The oldest sediments of unit U1 show a concave geometry downlapping towards the WSW and the ENE. There, unit U1 is deposited within a narrow passage between the steep flank of a coral bank, and a U2 scarp. In particular on the side of this scarp, large moat-like features (width up to 500 m) are observed (Figs 8–10). In some cases, they are filled with flat-topped acoustically transparent deposits (Figs 7 and 8), suggesting that these deposits could be turbidite deposits. The thickness of this mounded sediment body varies from 150 to 250 ms TWT. On the southwestern side of the coral bank, the thickness and reflector terminations are less pronounced, although subtle moats can be inferred.

The geometry and the reflectors of this sediment body suggest that the coral banks were already present before the deposition of unit U1, and that the coral banks were large and steep enough to intensify currents between their foot and the U2 scarp since the start of the deposition of unit U1. The oldest deposits of U1 are always observed in the centre of this passage from where they progressively prograded through time towards the flanks, creating a mounded geometry.

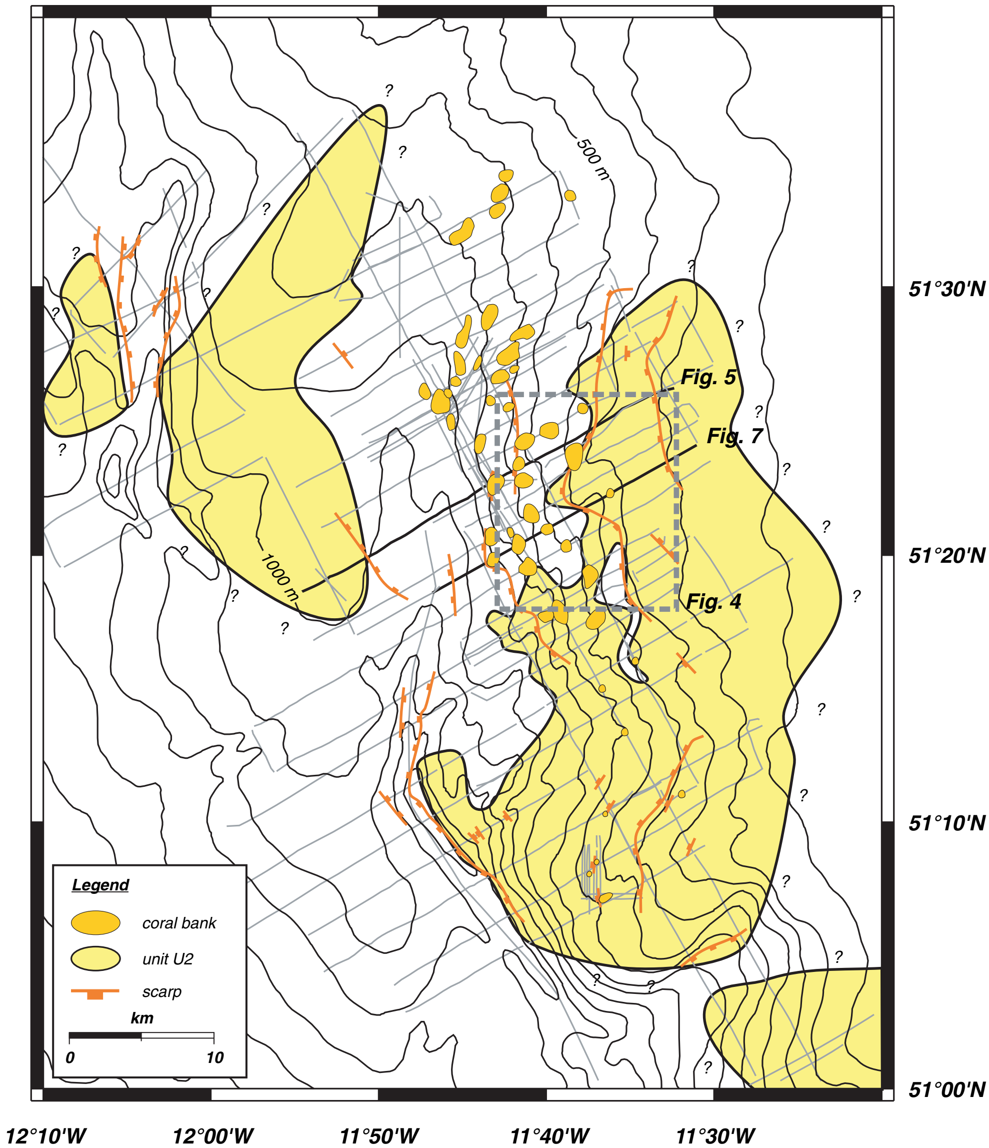

Fig. 6. Mapped distribution of seismic unit U2, the coral banks and the steep scarps created by the RD1 erosion event. All available high-resolution profiles are shown by grey lines.

After the passage became filled the reflectors started to onlap, but currents (still active, although possibly reduced in strength) created moats on both sides. This change is also accompanied by discontinuities on other seismic profiles. In a way, this drift shows similarities to mounded confined drifts such as the Louisville drift (Carter & McCave 1994), the Sicily channel drift (Marani *et al.* 1993) and the Sumba drift (Reed *et al.* 1987) as defined by Faugères *et al.* (1999). Confined drifts appear similar to elongate drifts, but are deposited in passages between tectonic or volcanic highs and are confined by boundary channels on both sides. In the BMP, however, this mounded drift is relatively small and it does not occur in a morpho-tectonically peculiar area such as the Louisville drift (Carter & McCave 1994). In this case, the narrow passage is constructed by an erosion event creating a scarp and by coral banks. Nevertheless, confined drifts remain very rare and this example

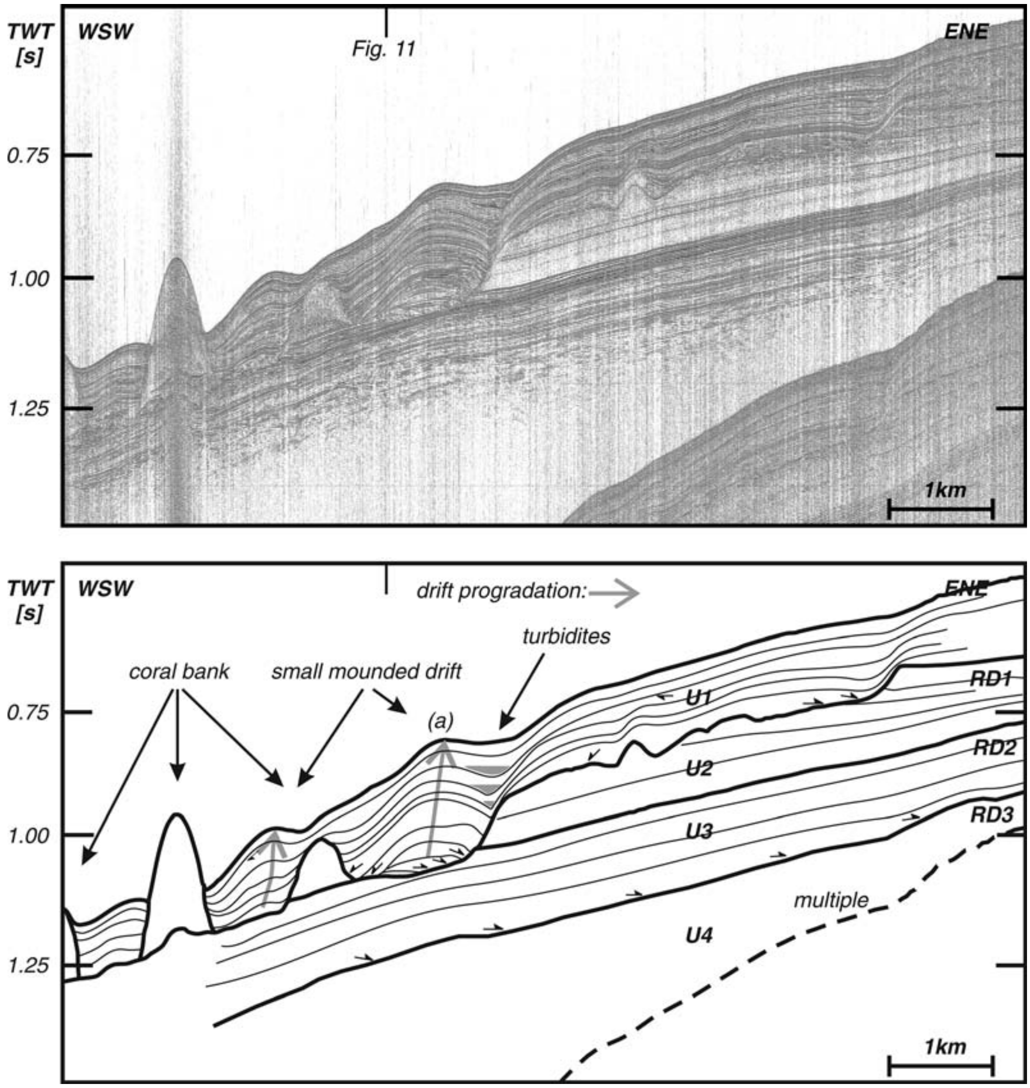

Fig. 7. Profile P010521, illustrating the general setting of the small mounded drift (a). West of the drift, an unconformity surface and a buried coral bank are rooted on the RD1 erosional surface. At its eastern edge, a steep scarp of unit U2 can be observed. The grey arrows indicate drift progradation. The gradual change in acoustic facies along the ENE side of unit U2 should be noted.

on one hand confirms their occurrence in peculiar areas, but on the other hand demonstrates that they do not need to be controlled in a pure morphotectonic way.

Core analyses

To further elucidate the true nature of the sediment drift deposits, two cores have been studied (Fig. 3). Core MD99-2327 (2625 cm long) was taken in a water depth of 651 m on the eastern flank of the sediment drift (Fig. 8) to provide an insight into the variability of the hydrodynamic environment. The site of core MD01-2449 (2215 cm long) is located in a water depth of 435 m, about 30 km SE of the sediment drift. Because of its location, it is out of range of the region of high bottom-current velocities. This rules out the possibility that the detrital and biogenic components would have been subject to major reworking through bottom currents.

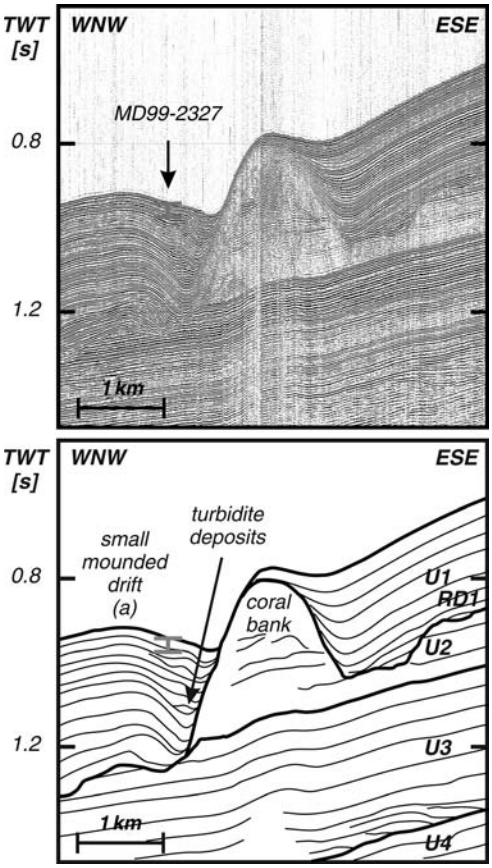

Fig. 8. Profile P010517, showing further detail of the MD99-2327 coring site, at the eastern flank of the small mounded drift.

This core should thus provide a continuous record of the regional palaeoclimatological signals.

Core MD99-2327 stratigraphy

Figure 12 illustrates the main characteristics of core MD99-2327. Although the sedimentary record is rather difficult to interpret in terms of chronostratigraphy, several features might characterize some key palaeoclimatological episodes. In particular, the magnetic susceptibility and the fraction $>150\ \mu m$ clearly show a significant change at about 1400 cm, subdividing the core into an upper and lower unit. A more detailed discussion concerning the atypical stratigraphy of this core has been given by Van Rooij *et al.* (2006).

From 0 to 1400 cm, the core contains homogeneous, olive grey silty clay with some sulphide strikes. At the base of this upper unit (1233–1425 cm), alternating layers of olive grey silty clay and muddy fine sand occur. The sediments are generally very poorly sorted, although sorting increases towards the base of this unit (Fig. 13). X-ray imagery reveals extensive bioturbation (mottling, planolites, chondrites, mycelia) throughout, varying from faint structures to very heavy burrowing (Van Rooij 2004). The upper unit is interpreted to record the last glacial period (Van Rooij *et al.* 2006). An indication of the presence of the cold MIS 4 is observed between 1000 and 1170 cm, with rather high values of NPS and $\delta^{18}O$ and by a rather low amount of coarse sand (Fig. 12). Two anomalies in NPS at 90 and 440 cm were dated respectively at 15.19 ± 0.13 ka BP and 17.38 ± 0.14 ka BP. These dates clearly reflect a gradual cooling with an abrupt culmination in NPS, $\delta^{18}O$ and density. X-ray imagery of these sections clearly shows higher concentrations of ice-rafted debris (IRD) in a heavily burrowed environment (Van Rooij 2004).

The lower unit, from 1500 to 2625 cm, is a very poorly to poorly sorted olive grey foraminiferal fine to medium sand (Fig. 13). Within these sediments occasional shell fragments, lithic grains and dark minerals are observed. Here, a higher sand percentage is present, and the magnetic susceptibility is lower (Fig. 12). Moreover, the $\delta^{18}O$ values also are lower and suggest, together with NPS, an interglacial environment (MIS 5) (Van Rooij *et al.* 2006). The exceptionally high amount of sand $>150\ \mu m$ cannot be interpreted in terms of ice-rafting events, but in terms of hydrodynamic activity.

Core MD01-2449 stratigraphy

The top part of this 2215 cm long core (0–26 cm) consists of olive clayey very fine quartz-foram sands. This grades downcore into olive grey to grey silty clays. Nannofossils and fine sand pockets were commonly observed in varying quantities. Two coarser-grained intervals were also observed; between 600 and 900 cm and between 1200 and 1400 cm. These two intervals are also characterized by elevated plateaux of dry bulk density (Fig. 14). A complete flow-in occurs below 2215 cm. As a consequence, only the first 22 m of this core were described. The variations in mainly dry bulk density, mean grain size, sand content (up to 20%) and magnetic susceptibility are similar to those of MD99-2327.

Common record of the two cores

The data presented here provide a first offshore record of the deglaciation history of the British–Irish Ice Sheet (BIIS). The characteristics and

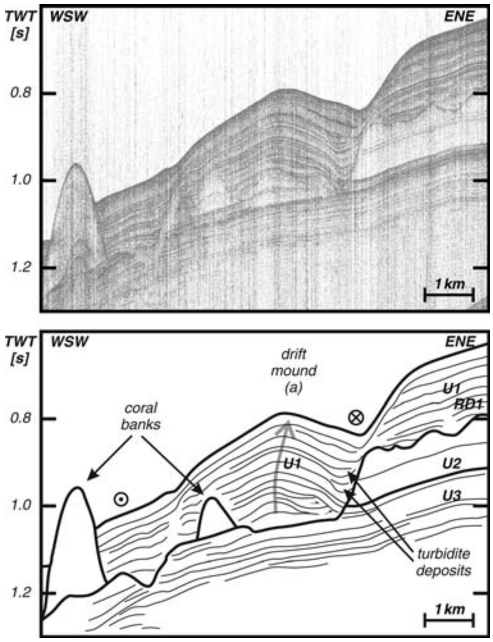

Fig. 9. Profile P980509, which makes a transect across the small mounded drift (a) in the central Belgica mound province. The mounded drift morphology occurs between the foot of a buried coral bank and a scarp in the flank of unit U2. The grey arrow indicates an upslope progradation of the crest of the drift mound. The moat indicating the pathway of a northward flowing current is filled with turbidite deposits.

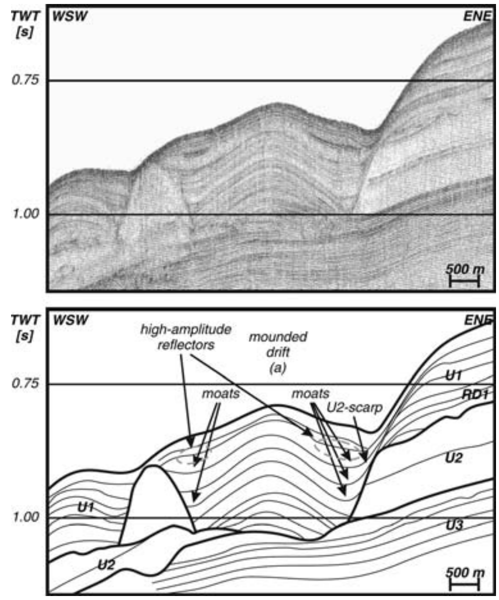

Fig. 10. Profile P970539, showing a typical cross-section of the drift mound within the Belgica mound province. On both sides, the moats show high-amplitude reflectors and probable turbidite deposits. The drift mound occurs between a large coral bank and the scarp in the U2 unit.

variations in dry bulk density, mean grain size and magnetic susceptibility of core MD01-2449 correlate with those of core MD99-2327 (Fig. 14). When the glacial records of the two cores are compared, it can be seen that the sedimentation rates at the site of MD01-2449 are significantly higher than those of the sediment drift site. This can be explained by the higher position on the slope of core MD01-2449 and by the sediment input coming from the Irish channel. This positive comparison strengthens and magnifies the sedimentary history of both cores, showing an atypical situation with a very local ice-rafting signature (Van Rooij *et al.* 2006).

The cold MIS 4 contains a relative minimum of IRD, suggesting a BIIS in a constructional stage with a period of falling sea level (Auffret *et al.* 2002). The high-variability record of IRD starts at about 62 ka (Fig. 13). All subsequent influx of terrigenous particles can be attributed to the BIIS destabilization. During MIS 3, the ice-rafting events succeed each other very closely and even grade smoothly into one another (Figs 13 and 14). This suggests that at the same time no other major sediment-supplying processes must have been active but ice-rafting, hemipelagic rain-out and limited lateral supply of bottom-current transported sediment.

However, with the start of MIS 2, an equal amount of IRD is delivered in a shorter time period compared with MIS 3. This episode of drastic increasing sedimentation rates reflects a higher variability of the BIIS destabilization and could be a record of a millennial-scale disintegration of the BIIS. McCabe & Clark (1998) and Knutz *et al*. (2001) considered the high frequency of BIIS-sourced IRD peaks to contribute to the millennial-scale pattern of iceberg discharges in the NE Atlantic. Several sources report two major shelf-edge advances and BIIS collapses from 26 to 18 ka and at 15 ka (Dowling & Coxon 2001; Knutz *et al*. 2002). These ages correspond to the ages of the two dated NPS anomalies. First of all, McCabe & Clark (1998) and Bowen *et al*. (2002) reported a significant deglaciation of the southern BIIS at about 17.4 ka. This could explain the two δ^{18}O meltwater peaks after 17.38 ka BP (at 400 cm). Moreover, the youngest event of 15.19 ka is consistent with the last collapse and also with the age of HE1 (15 ± 0.7 ka) of Elliot *et al*. (1998).

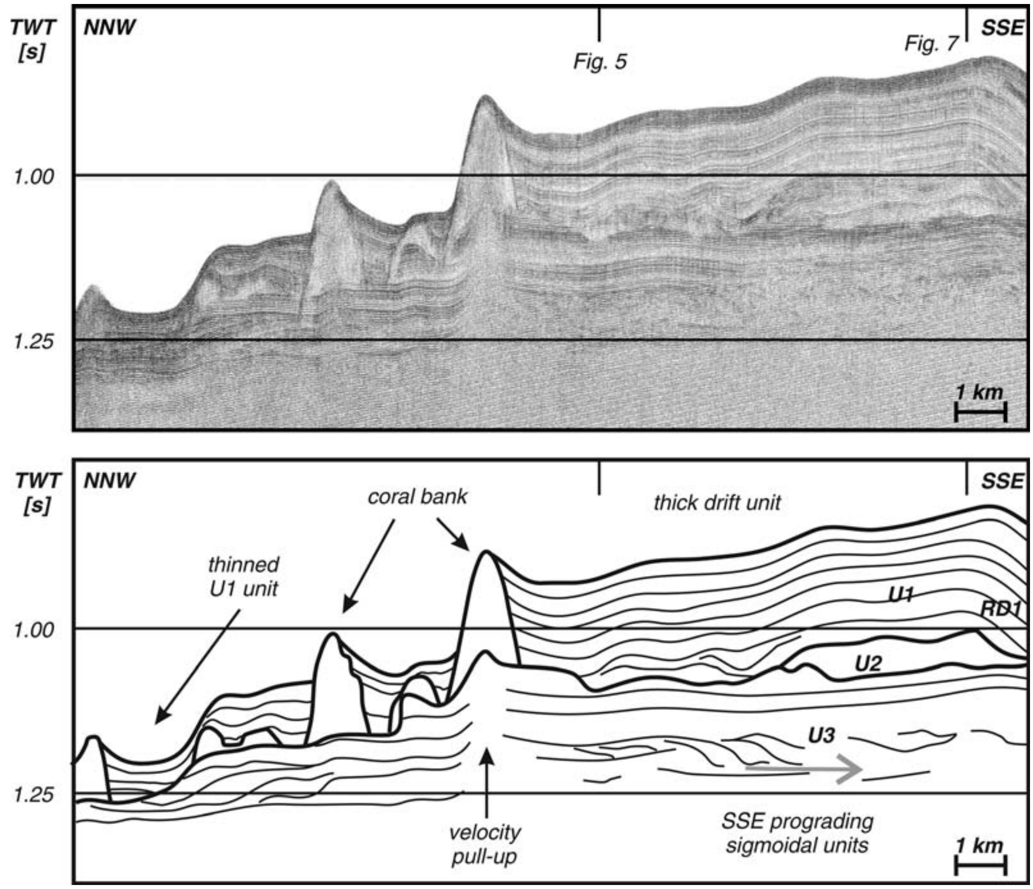

Fig. 11. Profile P980547, the only available alongslope profile crossing the sediment drift. It illustrates the variability of especially units U2 and U3. The marked change in sediment thickness south and north of the coral banks should be noted.

Hydrodynamic interpretation

The description of core MD99-2327 allows the recognition of two intervals, each of which can be interpreted in terms of a changing hydrodynamic environment. The most dominant feature of the glacial unit are the several episodes of ice-rafting events. The inferred IRD abundance is relatively high (5–10%). Particle size analysis shows, in general, that this unit is fine grained with a significantly high percentage of silt (65%), whereas clay tends to make up 8–24% of the sediments and the sand fraction is limited to an average of 18%. The total sample generally is very poorly sorted. The sortable silt index can provide estimates of current strength variations. Starting from the inferred MIS 4, five intervals of peak currents (28–33 μm) and five intervals of low currents (22–26 μm) are observed (Fig. 13). Transitions from minimum to maximum values on the sortable silt curve can be interpreted as accelerations of the bottom current, and vice versa. These peak current events (PCE) obviously behave in a more long-term way compared with the variations in the fraction >150 μm. It does not seem that the five peak current intervals coincide with significant ice-rafting intervals, suggesting another causal event. However, caution should be taken not to completely disconnect changes in sortable silt (thus benthic current variability) and the IRD (ice-rafting), because IRD also includes silt-sized particles. Most of the PCE peak during warm periods. Only PCE1 and partly PCE2 seem to be centred on a cold event. Probably, in this case, current-sorted silt and ice-rafted silt will be interfering factors. Because of the extensive bioturbation and burrowing, seen on X-ray imagery (Van Rooij 2004), it is very difficult to observe primary sedimentary

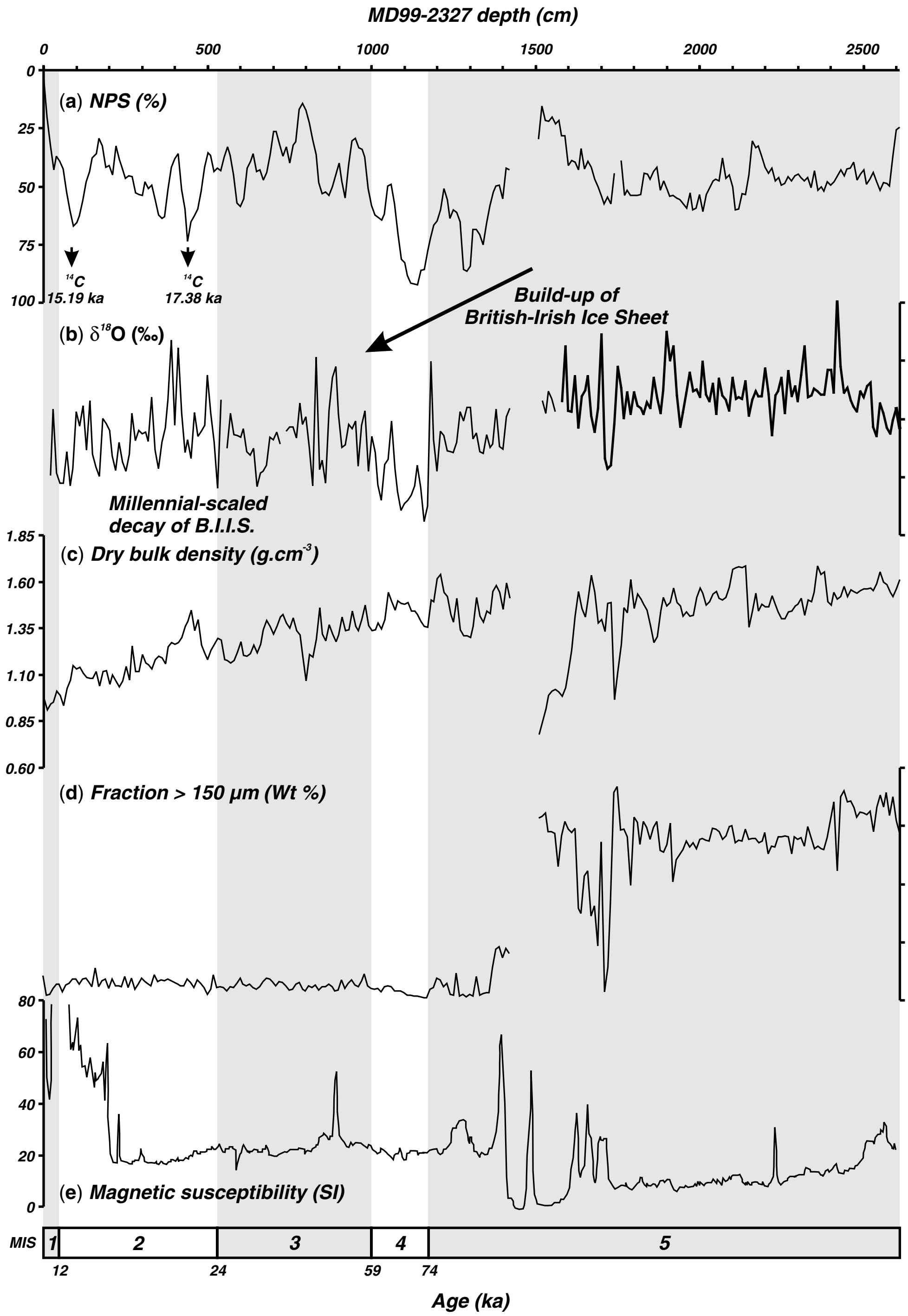

Fig. 12. Physical properties and stratigraphy of core MD99-2327 with (**a**) the relative abundance of the polar planktonic foraminifer *N. pachyderma s.* (%) (NPS (%)), (**b**) $\delta^{18}O$ stable isotopes (‰ v. PDB), (**c**) dry bulk density (g/cm^{-3}), (**d**) fraction >150 μm (wt%) and (**e**) the magnetic susceptibility. The grey-shaded areas highlight warmer (odd) marine isotope stages. The remarkable changes of (**d**) and (**e**) at about 14 m downcore should be noted.

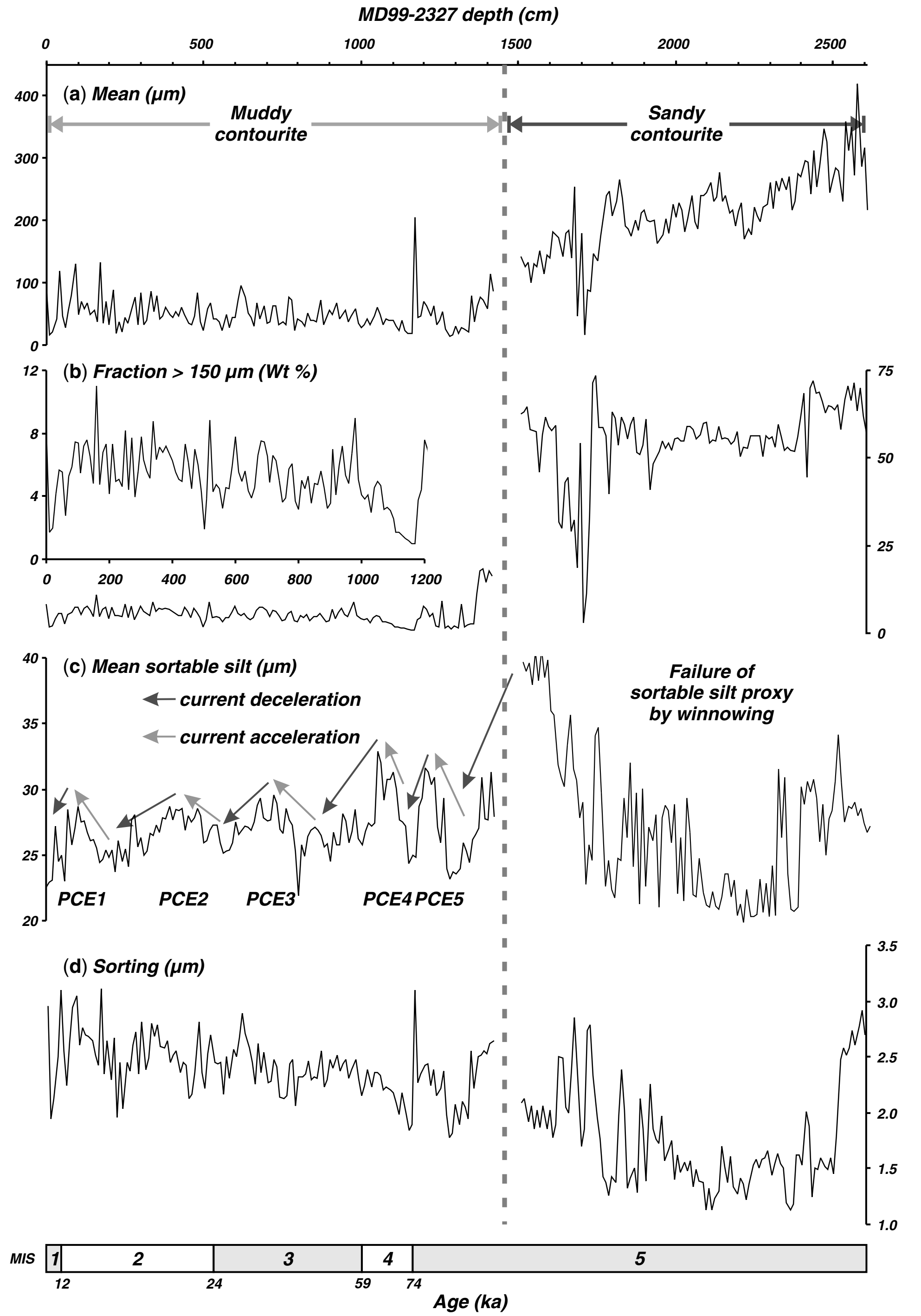

Fig. 13. Sedimentary processes and hydrodynamic interpretation of core MD99-2327 with (**a**) mean (µm), (**b**) fraction >150 µm (wt%), (**c**) mean sortable silt (µm) and (**d**) sorting (µm). Within (**b**), an inset of the glacial detail is provided. The five observed peak current episodes (PCE) are also presented.

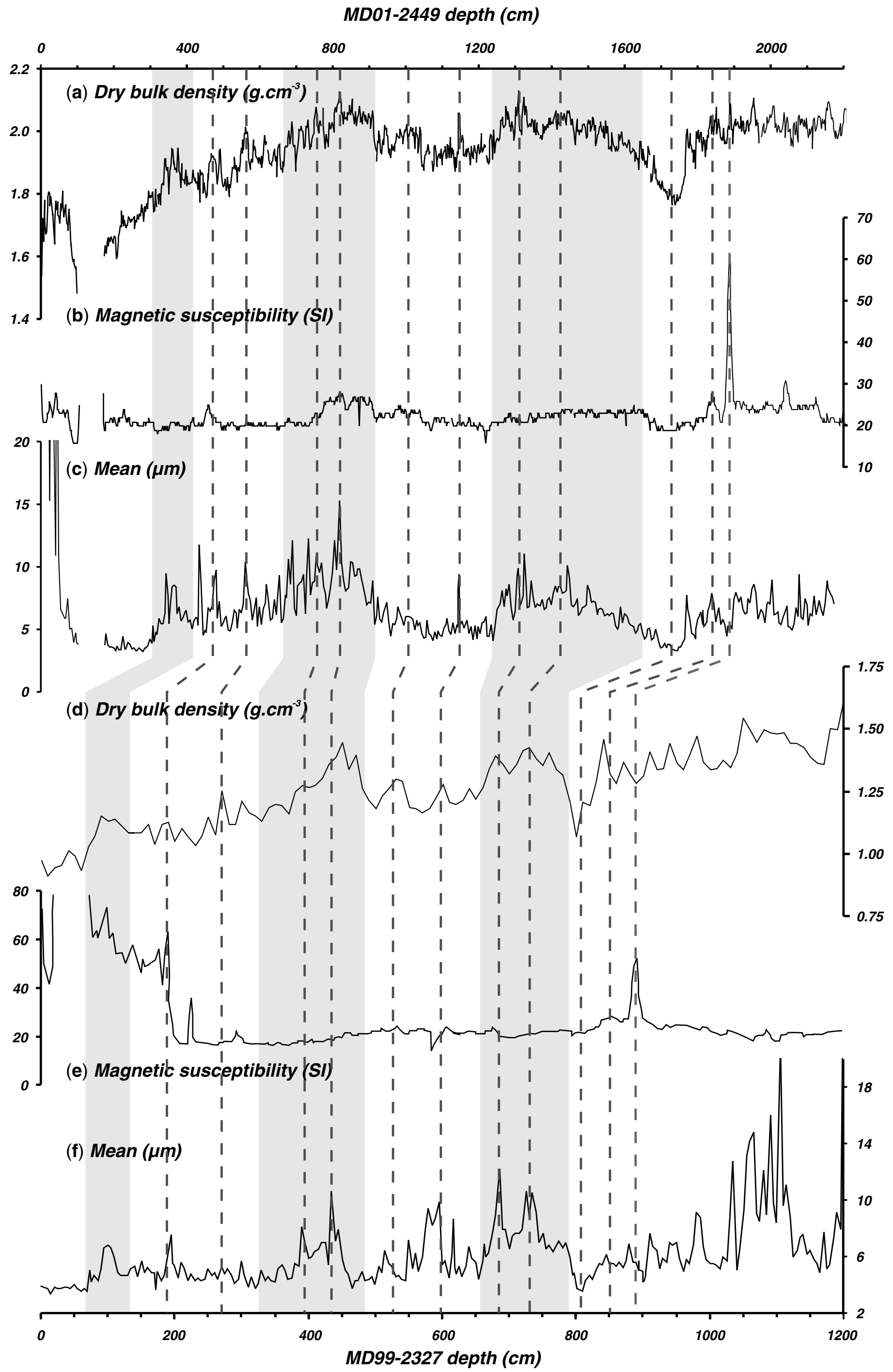

Fig. 14. Correlation of the glacial detail of core MD99-2327 with the higher-resolution data of core MD01-2449, based on respectively (**a**, **d**) dry bulk density (g cm^{-3}), (**b**, **e**) magnetic susceptibility (SI) and (**c**, **f**) mean grain size (µm). Specific correlation areas and points are indicated by grey-shaded areas or dashed lines, respectively.

structures. This bioturbation seems to be episodic and contains variations between mottling, isolated pockets and filaments. All this probably reflects several sediment sources in a biologically and hydrodynamically active area: current-sorted mud, biogenic components and ice-rafted debris.

Conversely, the sand percentage of the lower part of the core is up to 95% (with an average of 84%) and contains mostly quartz grains, detrital carbonate grains, and a high percentage of (reworked) planktonic and benthic foraminifers, reflecting a high biogenic productivity (Figs 12 and 13). This would also explain the large scatter in the oxygen isotope records, which indicates that (some of the) forams were reworked. These sediments are more sorted compared with the overlying units (although they still are poorly sorted), suggesting a significant benthic current influence. However, the sortable silt proxy cannot be applied in this part of the core because of the very low content of silt, which probably has been winnowed by strong currents. An alternative proxy for this benthic current strength can be suggested to be the mean of the 63–150 μm fraction, which encompasses the majority of the sediment, but excludes grains larger than 150 μm, whose origin is more likely to be related to ice-rafting. An increase in this sortable sand index as a result of increasing currents corresponds to a coarsening as the finer components are winnowed. This trend also corresponds to an increase in the degree of sorting, although mostly a fine tail remains present. As such, several fluctuations in current strength can be observed during the interglacial unit, with peak currents within the central part.

Discussion

The Quaternary hydrodynamic environment

Many observations on and around the area of the small mounded drift prove a very active hydrodynamic environment at present. Similar thin surface veneers also were observed on the Hebridean shelf and was interpreted as a contourite sand sheet (Armishaw *et al.* 2000; Akhurst *et al*. 2002). This requires the presence of a relatively strong, semi-permanent benthic current at intermediate depths at a velocity of over $30\ \mathrm{cm\ s^{-1}}$. The measured and inferred bottom-current velocities within the BMP are consistent with the requirements of Stow *et al*. (2002) for contourites, which involve an average current velocity of 10–$20\ \mathrm{cm\ s^{-1}}$ that can be accelerated up to $100\ \mathrm{cm\ s^{-1}}$ or more near steep slopes or narrow passageways. The required sediment supply zone can be variable, with upstream erosion, pirating and winnowing of slope sands (Armishaw *et al.* 2000). In this case, several sources are probable. The sedimentary analyses show that the entire core consists of contourites. The glacial unit meets many of the conditions of the muddy contourite facies as defined by Rebesco & Stow (2001) and Stow *et al*. (2002), although this is combined with a strong ice-rafting component. First, the sediment mainly consists of a siliciclastic fine-grained muddy silt. Indications for a mean grain size have been given by Stow & Piper (1984), who suggested 5–40 μm as a range for muddy contourites. Also, a sand percentage of 10–15% is inferred, but in this case, caution is necessary because a significant part of the sand content originated from ice-rafting. Only sporadically can primary structures be found; most of the core is structureless. The X-ray imagery confirms extensive bioturbation with (sulphide) filaments, planolites, mycelia and chondrites burrows. The nature of the bioturbation, and especially that of the filaments, seems to be variable within the core.

All analyses indicate that the nature and characteristics of the interglacial unit are similar to those of sandy contourites. Generally, they are a mixture of a terrigenous and biogenic content with evidence of abrasion and fragmental bioclasts (Faugères & Stow 1993; Stow *et al*. 2002). A very thick bedded, structureless coarse-grained deposit such as this one is extremely rare in this kind of environment and can, according to Stow & Mayall (2000), be classified as a deep-water massive sand. Mostly these are interpreted as sandy debris flows, although these sands can originate from various processes. In this case, many parameters indicate that the possibility that these interglacial sediments are mass-wasting deposits is rather small. Moreover, Figure 8 does not display features characteristic for a large debris flow or turbidite deposit. The general characteristics of such a deep-water massive sand were defined by Stow & Johansson (2000) and agree with the characteristics of the MIS 5 sediments. They are poorly to moderately sorted and have a high degree of reworking. Examples of sandy contourites as deep-water massive sands are rare and are found in morphologically and hydrodynamically special environments with fluctuating enhanced currents such as near the Gulf of Cadiz (Habgood *et al*. 2003) and the Sicilian gateway (Stow & Johansson 2000). Moreover, the massive (4.4 m) contourite sand deposits described by Habgood *et al*. (2003), have many similarities to the inferred contourite sands in core MD99-2327. In general, the size of a sandy contourite or a deep-water massive sand reported until now is rarely bigger than 1 m (Stow & Johansson 2000). Within this morphological and sedimentary context the presence of a 10 m thick sandy contourite is unique and requires further research.

Although no simple global response to climate can be found in bottom-current activity, it is very likely that the switch from a sandy to a muddy contouritic environment is associated with a particular palaeoclimatological change. Faugères & Stow (1993) linked a glacial dampened bottom-current regime to the presence of sea ice, whereas climate instability means enhanced bottom-current activity. Akhurst *et al*. (2002) have recently describe the presence of sandy contourites on the Hebrides slope during interglacials and interstadials and related them to enhanced current activity. They also recognized the presence of bottom-current action during glacial times, but less intense. This probably also is the case in our study area. Because the presence of enhanced currents in the BMP is highly dependent on the interaction with the MOW (New *et al.* 2001; De Mol *et al*. 2002; White 2006), it is plausible that glacial times seriously weaken the current regime to a muddy contourite sedimentation. The reduced outflow of MOW was then restricted to the Gulf of Cadiz and did not penetrate any further in the Atlantic Ocean (Schönfeld & Zahn 2000), so the conditions for enhanced currents were not met. The variability within the glacial contourite, however, is less clear. The inferred PCE are coeval with presumed warmer periods. During a climatic warmer period, the sea level could be more elevated, especially after a pan-Atlantic ice-rafting event. This could encourage an enhanced MOW production, which also could reach further into the Atlantic Ocean and create weak pulses of enhanced currents within the PSB.

A PSB contourite

The sedimentological record of this site demonstrates that the sediment body located between the coral banks and the steep flank of seismic unit U2 can be classified as a confined drift. The sedimentary facies suggests that the entire unit is influenced by fluctuating current intensities and thus the entire unit can be called a contourite drift at mid-water range (Stow *et al*. 2002). The sediment body shows many similarities to well-known contourite drift systems, such as a downcurrent elongation, subregional discontinuities and subparallel moderate- to low-amplitude reflectors with gradual change in seismic facies (Faugères *et al*. 1999; Rebesco & Stow 2001). Compared with the dimensions of published contourite drifts, the confined drift in the Porcupine Seabight is one of the smaller ones (*c*. 50 km^2). The few other examples of this type of drift are known within small basins (Stow *et al*. 2002), but are much larger. The best comparison can be made with the Sumba drift (Sunda Arc, Indonesia); a smooth asymmetric mound with boundary channels and sandy contourites (15 km elongation) (Reed *et al*. 1987). As a result of lateral current velocity gradients within the Sumba drift, muddy contourites were deposited on the central part and sandy contourites in boundary channels. However, the Sumba confined drift is 15 km wide, whereas our equivalent is only 4 km wide. It could thus be possible that lateral facies changes are less pronounced in the PSB small mounded drift and such changes can only be observed in depth (or time). The nature of the bathymetric restrictions that are responsible for the acceleration of deep currents, however, are of a completely different nature and are at the base of the smaller dimension. Whereas the Sumba drift and other confined drifts have a more tectonically controlled background, the interaction between water-mass mixing and bathymetric interaction is steered in this case by a combination of a turbulent sedimentary history with several erosion episodes and current-controlled biogenic build-ups. Within such a dynamic and irregular environment, it is expected that, besides contourites, turbiditic and other mass-wasting deposits can also be inferred.

The characteristics of the lower drift strata suggest a significant period of non-sedimentation between the onset of coral bank growth in the Late Pliocene and the onset of drift sedimentation. This period of non-sedimentation gives enough time for the ‘start-up’ phase of the coral bank, required by De Mol *et al*. (2002) for corals to settle on the hard substratum provided by the bottom-current swept and eroded U2 unit. From a palaeoceanographic point of view, we could imagine that the contouritic sedimentation was well under way during a major climatological change within the Pleistocene. The Mid-Pleistocene revolution (MPR, *c*. 940–640 ka) marks the change towards an increasing mean global ice volume and increasing amplitude of 100 ka climatological cycles (Raymo *et al.* 1997; Hernandez-Molina *et al*. 2002). This interval was also characterized by ‘weaker’ NADW formation, relative to the early and late Pleistocene (Raymo *et al*. 1997). On the other hand, after the MPR the pulsations between glacial and interglacial periods became more pronounced. They could be the cause of the start of the muddy–sandy contourite deposition in the BMP, as well as the acoustic amplitude variations within seismic unit U1.

Within the BMP, the presence of this small mounded drift is a common feature everywhere that the palaeotopography and the presence of the coral banks allow a similar setting. Sidescan sonar imagery of the entire province proves that in a similar depth-range and within the vicinity of the coral banks, enhanced currents are almost always inferred; thus, a similar build-up of hydrodynamic variability through time can be expected. However, as the presence of the current enhancement is strictly bound to the water mass–topography interaction in this region on the slope, we conclude that the presence of this confined contourite drift is a very local feature, bound to several geological, climatological, biological and hydrodynamic variables.

Conclusion

The Belgica mound province, located on the eastern slope of the Porcupine Seabight, is considered a unique environment within the North Atlantic domain because of its particular hydrographic, geological and morphological settings associated with the presence of deep-water coral banks. This paper demonstrates that, since the Neogene, strong northward-flowing currents on this part of the margin were responsible for the deposition of bottom-current controlled deposits (Fig. 15a).

Seismic interpretation of 1500 km of high-resolution seismic profiles across this coral bank province shows that after the deposition of the acoustically transparent unit U2 with as yet unknown lithology, the regional unconformity RD1 (recording a major change in oceanographic conditions) was responsible for the removal of a large part of this unit in the Late Pliocene (Fig. 15b). This unconformity also marks the start of glacial–interglacial cycles and their effects on the deep-water circulation. Subsequent to the RD1 event, corals began to settle on topographic irregularities in the palaeobathymetry. The coral banks were built spectacularly fast in a period when the adjacent areas experienced non-deposition. They are located in a zone within the influence of a complex system of enhanced currents, which is believed to be the main driving force of the controls on their development.

Towards a later phase of the Pleistocene, when the glacial and interglacial periods began to shift towards a 100 ka frequency, a vigorous bottom-current regime was installed and deposited small contouritic deposits closely related to almost full-grown coral banks (Fig. 15c). The special setting of this sediment body, the morphology of which has been influenced by the presence of the coral banks and the underlying palaeotopography, makes this drift probably one of the smallest known confined contourite drifts (Fig. 15d). Side-scan sonar imagery has already proved the presence of a sandy contourite sheet with sand waves over a large part of the confined contourite drift. This Holocene sandy contourite shares many characteristics with the interglacial part of core MD99-2327, located between 1500 and 2625 cm. During this period, we can infer an environmental situation similar to that at present. This entire unit can be considered as a sandy contourite and also one of the largest known deep-water massive sands.

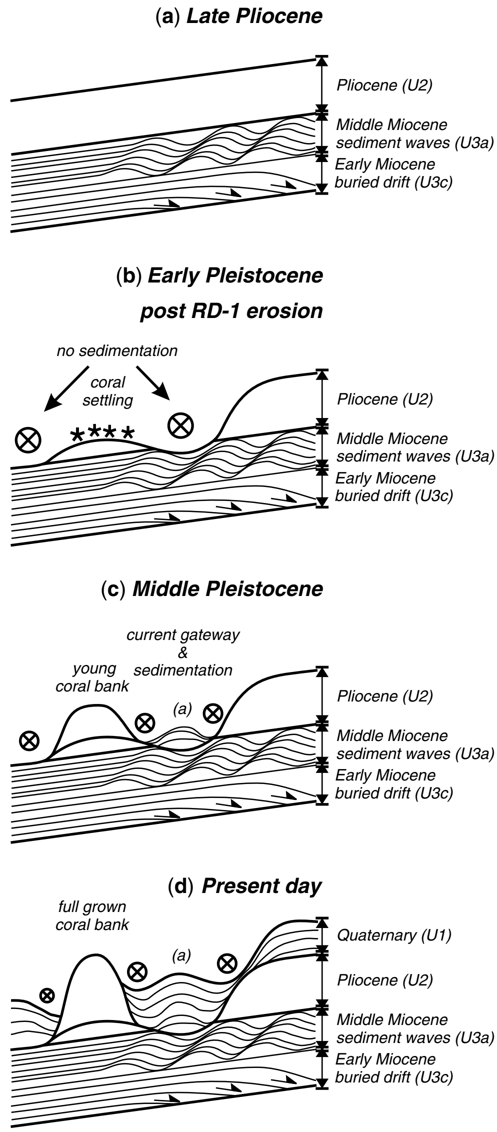

Fig. 15. Reconstruction of the depositional evolution, in an idealized SW–NE section, of the small confined contourite drift (a) in relation to the growth of a coral bank. The crossed circles illustrate the presence of a northward-flowing current.

During the transition from isotope stage 5 to stage 4, the accumulating ice volumes of the pan-Atlantic ice sheets were responsible for a global sea-level drop and the distribution of the MOW in the Eastern Atlantic was seriously hampered. Because the presence of the MOW was vital to the vigorous BMP hydrodynamic environment, the activity of the glacial bottom currents was reduced. However, evidence of current reactivation, coupled with warmer periods, suggests that enough MOW sporadically entered the Porcupine Seabight to briefly enhance the bottom-current production. This glacial part of the core is a typical muddy contourite with a significant glacio-marine contribution.

Within this relatively small embayment in the NE Atlantic margin, typical features diagnostic of sediment drifts are encountered. The key factors allowing the construction of this contourite system are unique because they result from the interaction between a complex hydrographic system confined by obstacles in the palaeobathymetry, located in a relatively narrow zone of the slope. Evidently, this also calls for a more genetic nomenclature, indicating the causal mechanisms and depth ranges of the contourite deposits. Additionally, this example also proves that the location of this drift seems to be ideal to monitor the changes of the palaeoclimate and palaeoceanography record off Ireland.

This study of deep-sea sediment dynamics within the Porcupine Seabight was carried out within the framework of the EC FP5 programmes ECOMOUND and GEOMOUND and the Ghent University project 'GOA Porcupine–Belgica'. Core MD99-2327 has been acquired under the IMAGES programme. Support is gratefully acknowledged from the Ghent University Palaeontology Department (S. Louwye, S. Van Cauwenberghe) and the Marine Biology Section (M. Vinckx, D. Van Gansbeke and D. Schram) for laboratory use. We would also like to thank the captains and crews of R. V. *Belgica* and R. V. *Marion Dufresne*. The constructive suggestions of S. Ceramicola and B. De Mol significantly improved the manuscript. D.V.R. is a post-doctoral fellow funded by the FWO Flanders.

References

AKHURST, M. C., STOW, D. A. V. & STOKER, M. S. 2002. Late Quaternary glacigenic contourite, debris flow and turbidite process interaction in the Faroe–Shetland Channel, NW European Continental Margin. *In*: STOW, D. A. V., PUDSEY, C. J., HOWE, J. A., FAUGÈRES, J.-C. & VIANA, A. R. (eds) *Deep-Water Contourite Systems: Modern Drifts and Ancient Series, Seismic and Sedimentary Characteristics*. Geological Society, London, Memoirs, **22**, 73–84.

ARMISHAW, J. E., HOLMES, R. W. & STOW, D. A. V. 2000. The Barra Fan: a bottom-current reworked, glacially-fed submarine fans system. *Marine and Petroleum Geology*, **17**, 219–238.

AUFFRET, G. A., ZARAGOSI, S., DENNIELOU, B., *ET AL.* 2002. Terrigenous fluxes at the Celtic margin during the last glacial cycle. *Marine Geology*, **188**, 79–108.

BARD, E. 1998. Geochemical and geophysical implications of the radiocarbon calibration. *Geochimica et Cosmochimica Acta*, **62**, 2025–2038.

BOWEN, D. Q., PHILLIPS, F. M., MCCABE, A. M., KNUTZ, P. C. & SYKES, G. A. 2002. New data for the Last Glacial Maximum in Great Britain and Ireland. *Quaternary Science Reviews*, **21**, 89–101.

CARTER, L. & MCCAVE, I. N. 1994. Late Quaternary sediment pathways through the deep ocean, east of New Zealand. *Paleoceanography*, **9**, 1061–1085.

DE MOL, B., VAN RENSBERGEN, P., PILLEN, S., *ET AL.* 2002. Large deep-water coral banks in the Porcupine Basin, southwest of Ireland. *Marine Geology*, **188**, 193–231.

DOWLING, L. A. & COXON, P. 2001. Current understanding of Pleistocene temperate stages in Ireland. *Quaternary Science Reviews*, **20**, 1631–1642.

EDIGER, V., VELEGRAKIS, A. F. & EVANS, G. 2002. Upper slope sediment waves in the Cilician Basin, northeastern Mediterranean. *Marine Geology*, **192**, 321–333.

ELLIOT, M., LABEYRIE, L. D., BOND, G., CORTIJO, E., TURON, J.-L., TISNERAT, N. & DUPLESSY, J. C. 1998. Millennial-scale iceberg discharges in the Irminger Basin during the last glacial period: relationship with the Heinrich events and environmental settings. *Paleoceanography*, **13**, 433–446.

FAUGÈRES, J.-C. & STOW, D. A. V. 1993. Bottom-current-controlled sedimentation: a synthesis of the contourite problem. *Sedimentary Geology*, **82**, 287–297.

FAUGÈRES, J.-C., STOW, D. A. V., IMBERT, P. & VIANA, A. R. 1999. Seismic features diagnostic of contourite drifts. *Marine Geology*, **162**, 1–38.

FOUBERT, A., BECK, T., WHEELER, A. J., *ET AL.* 2005. New view of the Belgica Mounds, Porcupine Seabight, NE Atlantic: preliminary results from the *Polarstern* ARK-XIX/3a ROV cruise. *In*: FREIWALD, A. & ROBERTS, J. M. (eds) *Deep-water Corals and Ecosystems*. Springer, Heidelberg, 403–415.

FREIWALD, A., WILSON, J. B. & HENRICH, R. 1999. Grounding Pleistocene icebergs shape recent deep-water coral reefs. *Sedimentary Geology*, **125**, 1–8.

HABGOOD, E., KENYON, N. H., MASSON, D. G., AKHMETZHANOV, A. M., WEAVER, P. P. E., GARDNER, J. & MULDER, T. 2003. Deep-water sediment wave fields, bottom current sand channels and gravity flow channel-lobe systems: Gulf of Cadiz, NE Atlantic. *Sedimentology*, **50**, 483–510.

HARGREAVES, P. M. 1984. The distribution of Decapoda (Crustacea) in the open ocean and near-bottom over an adjacent slope in the northern North-East Atlantic Ocean during Autumn 1979. *Journal of the Marine Biological Association of the United Kingdom*, **64**, 829–857.

HENRIET, J.-P., DE MOL, B., PILLEN, S., *ET AL.* 1998. Gas hydrate crystals may help build reefs. *Nature*, **391**, 648–649.

HERNANDEZ-MOLINA, F. J., SOMOZA, L., VAZQUEZ, J. T., LOBO, F., FERNANDEZ-PUGA, M. C., LLAVE, E. & DIAZ-DEL RIO, V. 2002. Quaternary stratigraphic stacking patterns on the continental shelves of the southern Iberian Peninsula: their relationship with global climate and palaeoceanographic changes. *Quaternary International*, **92**, 5–23.

HUVENNE, V., BLONDEL, P. & HENRIET, J.-P. 2002. Textural analyses of sidescan sonar imagery from two mound provinces in the Porcupine Seabight. *Marine Geology*, **189**, 323–341.

HUVENNE, V. A. I., DE MOL, B. & HENRIET, J.-P. 2003. A 3D seismic study of the morphology and spatial distribution of buried coral banks in the Porcupine Basin, SW of Ireland. *Marine Geology*, **198**, 5–25.

KENYON, N. H., IVANOV, M. K., AKHMETZHANOV, A. M. & NEW, A. L. 1998. The current swept continental slope and giant carbonate mounds to the West of Ireland. *In*: DE MOL, B. (ed.) *Geosphere–Biosphere Coupling: Carbonate Mud Mounds and Cold Water Reefs*. IOC Workshop Report, **143**, 24.

KNUTZ, P. C., AUSTIN, W. E. N. & JONES, E. J. W. 2001. Millennial-scaled depositional cycles related to British Ice Sheet variability and North Atlantic paleocirculation since 45 kyr B.P., Barra Fan, U.K. margin. *Paleoceanography*, **16**, 53–64.

KNUTZ, P. C., HALL, I. R., ZAHN, R., RASMUSSEN, T., KUIJPERS, A., MOROS, M. & SHACKLETON, N. J. 2002. Multidecadal ocean variability and NW European ice sheet surges during the last deglaciation. *Geochemistry, Geophysics, Geosystems*, **3**, 1077.

MARANI, M., ARGNANI, A., ROVERI, M. & TRINCARDI, F. 1993. Sediment drifts and erosional surfaces in the central Mediterranean: seismic evidence of bottom-current activity. *Sedimentary Geology*, **82**, 207–220.

MCCABE, A. M. & CLARK, P. U. 1998. Ice-sheet variability around the North Atlantic Ocean during the last deglaciation. *Nature*, **392**, 373–377.

MCCAVE, I. N., MANIGHETTI, B. & ROBINSON, S. G. 1995. Sortable silt and fine sediment size/composition slicing: parameters for palaeocurrent speed and palaeoceanography. *Paleoceanography*, **10**, 593–610.

MOORE, J. G. & SHANNON, P. M. 1991. Slump structures in the Late Tertiary of the Porcupine Basin, offshore Ireland. *Marine and Petroleum Geology*, **8**, 184–197.

NEW, A. L., BARNARD, S., HERRMANN, P. & MOLINES, J.-M. 2001. On the origin and pathway of the saline inflow to the Nordic Seas: insights from models. *Progress in Oceanography*, **48**, 255–287.

PEARSON, I. & JENKINS, D. G. 1986. Unconformities in the Cenozoic of the North-East Atlantic. *In*: SUMMERHAYES, C. P. & SHACKLETON, N. J. (eds) *North Atlantic Palaeoceanography*. Geological Society, London, Special Publications, **21**, 79–86.

PINGREE, R. D. & LE CANN, B. 1989. Celtic and Armorican slope and shelf residual currents. *Progress in Oceanography*, **23**, 303–338.

PINGREE, R. D. & LE CANN, B. 1990. Structure, strength and seasonality of the slope currents in the Bay of Biscay region. *Journal of the Marine Biological Association of the United Kingdom*, **70**, 857–885.

POLLARD, R. T., GRIFFITHS, M. J., CUNNINGHAM, S. A., READ, J. F., PÉREZ, F. F. & RIOS, A. F. 1996. Vivaldi 1991—a study of the formation, circulation and ventilation of Eastern North Atlantic Central Water. *Progress in Oceanography*, **37**, 167–172.

RAYMO, M. E., OPPO, D. & CURRY, W. B. 1997. The mid-Pleistocene climate transition: a deep sea carbon isotopic perspective. *Paleoceanography*, **12**, 546–559.

REBESCO, M. & STOW, D. A. V. 2001. Seismic expression of contourites and related deposits: a preface. *Marine Geophysical Researches*, **22**, 303–308.

REED, D. L., MEYER, A. W., SILVER, E. A. & PRASETYO, H. 1987. Contourite sedimentation in an intraoceanic forearc system: eastern Sunda Arc, Indonesia. *Marine Geology*, **76**, 223–242.

RICE, A. L., THURSTON, M. H. & NEW, A. L. 1990. Dense aggregations of a hexactinellid sponge, *Pheromena carpenteri*, in the Porcupine Seabight (northeast Atlantic Ocean), and possible causes. *Progress in Oceanography*, **24**, 179–196.

RICE, A. L., BILLET, D. S. M., THURSTON, M. H. & LAMPITT, R. S. 1991. The Institute of Oceanographic Sciences Biology programme in the Porcupine Seabight: background and general introduction. *Journal of the Marine Biological Association of the United Kingdom*, **71**, 281–310.

SCHÖNFELD, J. & ZAHN, R. 2000. Late Glacial to Holocene history of the Mediterranean Outflow. Evidence from benthic foraminiferal assemblages and stable isotopes at the Portuguese margin. *Palaeogeography, Palaeoclimatology, Palaeoecology*, **159**, 85–111.

STOW, D. A. V. 1982. Bottom currents and contourites in the North Atlantic. *Bulletin de l'Institut de Géologie du Bassin d'Aquitaine*, **31**, 151–166.

STOW, D. A. V. & JOHANSSON, M. 2000. Deep-water massive sands: nature, origin and hydrocarbon implications. *Marine and Petroleum Geology*, **17**, 145–174.

STOW, D. A. V. & MAYALL, M. 2000. Deep-water sedimentary systems: new models for the 21st century. *Marine and Petroleum Geology*, **17**, 125–135.

STOW, D. A. V. & PIPER, D. J. W. 1984. Deep-water fine-grained sediments: facies models. *In*: STOW, D. A. V. & PIPER, D. J. W. (eds) *Fine-Grained Sediments, Deep-Water Processes and Facies*. Geological Society, London, Special Publications, **15**, 611–646.

STOW, D. A. V., FAUGÈRES, J.-C., HOWE, J. A., PUDSEY, C. J. & VIANA, A. R. 2002. Bottom currents, contourites and deep-sea sediment drifts: current state-of-the-art. *In*: STOW, D. A. V., PUDSEY, C. J., HOWE, J. A., FAUGÈRES, J.-C. & VIANA, A. R. (eds) *Deep-Water Contourite Systems: Modern Drifts and Ancient Series,* *Seismic and Sedimentary Characteristics*. Geological Society, London, Memoirs, **22**, 7–20.

VAN AKEN, H. M. 2000. The hydrography of the mid-latitude northeast Atlantic Ocean I. *Deep-Sea Research I*, **47**, 757–788.

VAN ROOIJ, D. 2004. *An integrated study of Quaternary sedimentary processes on the eastern slope of the Porcupine Seabight, SW of Ireland*. PhD thesis, Ghent University.

VAN ROOIJ, D., DE MOL, B., HUVENNE, V., IVANOV, M. K. & HENRIET, J.-P. 2003. Seismic evidence of current-controlled sedimentation in the Belgica mound province, upper Porcupine slope, southwest of Ireland. *Marine Geology*, **195**, 31–53.

VAN ROOIJ, D., BLAMART, D., RICHTER, T., WHEELER, A., KOZACHENKO, M. & HENRIET, J.-P. 2006. Quaternary sediment dynamics in the Belgica mound province, Porcupine Seabight: ice rafting events and contour current processes. *International Journal of Earth Sciences*, doi: 10.1007/s00531-006-0068-6.

WHEELER, A. J., BETT, B. J., BILLET, D. S. M. & MASSON, D. G. 2000. Very high resolution side-scan mapping of deep-water coral mounds: surface morphology and processes affecting growth. *EOS Transactions*, *American Geophysical Union*, **81**, 48.

WHITE, M. 2006. The hydrographic setting for the carbonate mounds of the Porcupine Bank and Sea Bight. *International Journal of Earth Sciences*, doi: 10.1007/s00531-006-0099-1.

WHITE, M., MOHN, C., DE STIGTER, H. & MOTTRAM, G. 2005. Deep-water coral development as a function of hydrodynamics and surface productivity around the submarine banks of the Rockall Trough, NE Atlantic. *In*: FREIWALD, A. & ROBERTS, J. M. (eds) *Deep-water Corals and Ecosystems*. Springer, Heidelberg, 503–514.